Severity of Diabetes Governs Vascular Lipoprotein Lipase by Affecting Enzyme Dimerization and Disassembly

Ying Wang, Prasanth Puthanveetil, Fang Wang, Min Suk Kim, Ashraf Abrahani, and Brian Rodrigues

OBJECTIVE—In diabetes, when glucose consumption is restricted, the heart adapts to use fatty acid (FA) exclusively. The majority of FA provided to the heart comes from the breakdown of circulating triglyceride (TG), a process catalyzed by lipoprotein lipase (LPL) located at the vascular lumen. The objective of the current study was to determine the mechanisms behind LPL processing and breakdown after moderate and severe diabetes.

RESEARCH DESIGN AND METHODS—To induce acute hyperglycemia, diazoxide, a selective, ATP-sensitive K^+ channel opener was used. For chronic diabetes, streptozotocin, a β-cell–specific toxin was administered at doses of 55 or 100 mg/kg to generate moderate and severe diabetes, respectively. Cardiac LPL processing into active dimers and breakdown at the vascular lumen was investigated.

RESULTS—After acute hyperglycemia and moderate diabetes, more LPL is processed into an active dimeric form, which involves the endoplasmic reticulum chaperone calnexin. Severe diabetes results in increased conversion of LPL into inactive monomers at the vascular lumen, a process mediated by FA-induced expression of angiopoietin-like protein 4 (Angptl-4).

CONCLUSIONS—In acute hyperglycemia and moderate diabetes, exaggerated LPL processing to dimeric, catalytically active enzyme increases coronary LPL, delivering more FA to the heart when glucose utilization is compromised. In severe chronic diabetes, to avoid lipid oversupply, FA-induced expression of Angptl-4 leads to conversion of LPL to inactive monomers at the coronary lumen to impede TG hydrolysis. Results from this study advance our understanding of how diabetes changes coronary LPL, which could contribute to cardiovascular complications seen with this disease. ***Diabetes*** **60:2041–2050, 2011**

Energy demand of the heart is met by oxidation of multiple substrates, which include glucose and fatty acids (FA) (1,2). The latter substrate is a favorite fuel, with almost 70% of ATP generated from oxidation of FA under normal conditions (3). However, based on their availability under different physiological and pathophysiological conditions, the heart can rapidly switch its substrate selection (4,5). In diabetes, when glucose consumption is restricted as a result of impaired glucose transport, glycolysis, and pyruvate oxidation, the heart adapts to use FA exclusively (2). Regrettably, this adjustment could be deleterious, since excess FA delivery leads to lipid overload (lipotoxicity), and eventually cardiomyopathy.

Exogenous FA are provided to the heart from FA bound to albumin or subsequent to breakdown of circulating triglyceride (TG)-rich lipoproteins by lipoprotein lipase (LPL) (6,7). This enzyme, bound to heparan sulfate proteoglycan (HSPG) binding sites, and strategically located at the vascular lumen side of endothelial cells, hydrolyzes TG to release FA (8). Endothelial cells do not express LPL (9). In the heart, LPL is synthesized and processed in cardiomyocytes, transported to myocyte cell-surface HSPGs, and eventually transported to the coronary lumen (10,11).

Studies from our laboratory have demonstrated a robust increase of coronary LPL in an animal model of moderate diabetes; these animals develop hyperglycemia without any change in circulating TG or FA (12–14). As the increase in LPL occurred in the absence of any change in gene expression in the whole heart, we hypothesized that LPL is regulated by post-transcriptional mechanisms. In this regard, we reported an augmented trafficking of LPL from the Golgi to the myocyte surface, and ultimately the vascular lumen (12,13,15). Notwithstanding this augmented trafficking, other posttranslational mechanisms could also play important roles in regulating LPL after diabetes. Catalytically active LPL at the vascular lumen is a homodimer, with two inactive monomeric subunits assembled noncovalently in a head-to-tail fashion (16–18). This assembly relies on processing in the endoplasmic reticulum (ER) and involves multiple steps, including early association with the ER-resident chaperones calnexin/calreticulin and subsequent dimerization facilitated by lipase maturation factor 1 (LMF1) (19–23). Association with calnexin/calreticulin allows nascent LPL folding into a proper tertiary structure qualified for dimerization; only dimeric LPL is active and competent to exit the ER, en route for secretion (19,20,22).

Compared with moderate diabetes, animals with severe diabetes demonstrate a decline in coronary LPL (13). As these animals exhibit elevated circulating FA in addition to hyperglycemia, we assumed that LPL-mediated FA delivery would be redundant, and hence is "turned off" (13). Mechanisms proposed for this decline in vascular LPL include impaired LPL vesicle transport, FA-induced displacement of enzyme from endothelial HSPGs, and direct inactivation of the enzyme by product inhibition (13,24,25). A newly identified member of the angiopoietin family, angiopoietin-like protein 4 (Angptl-4), could also be added to this list. Angptl-4 converts dimeric LPL into inactive monomers, thereby reducing LPL activity at the vascular lumen (26,27). It is possible that in severe diabetes, elevated circulating FA stimulates Angptl-4 expression, and eventually LPL inhibition. The objective of the current study was to determine the contribution of enzyme assembly and disassembly in regulating cardiac LPL activity after moderate and severe diabetes.

From the Faculty of Pharmaceutical Sciences, The University of British Columbia, Vancouver, British Columbia, Canada.
Corresponding author: Brian Rodrigues, rodrigue@interchange.ubc.ca.
Received 14 January 2011 and accepted 5 May 2011.
DOI: 10.2337/db11-0042
This article contains Supplementary Data online at http://diabetes.diabetesjournals.org/lookup/suppl/doi:10.2337/db11-0042/-/DC1.

RESEARCH DESIGN AND METHODS

Experimental animals. The investigation conforms to the Guide for the Care and Use of Laboratory Animals published by National Institutes of Health and the University of British Columbia. Adult male Wistar rats (250–320 g) were used. To induce acute hyperglycemia, diazoxide (DZ), a selective, ATP-sensitive K^+ channel opener was administered intraperitoneally at 100 mg/kg. DZ causes a rapid decrease of insulin secretion within 1 h, and the animals remain hyperglycemic for 4 h (28–30). Four hours after DZ, animals were killed and hearts were removed. For chronic diabetes, streptozotocin (STZ), a β-cell–specific toxin was administered as a single dose intravenously to more closely mimic type 1 diabetes (12,13). STZ was given at doses of 55 (D55) or 100 (D100) mg/kg. With D55, animals are insulin deficient but do not require insulin supplementation for survival (moderate diabetes). Unlike D55, D100 animals also develop hyperlipidemia and are not able to survive beyond 4 days without insulin supplementation (severe diabetes). STZ animals were kept for 4 days before hearts were removed.

Isolated heart perfusion. Hearts were isolated and perfused retrogradely (14). To measure coronary LPL, perfusion solution was changed to buffer containing heparin (5 units/mL). Perfusion effluent was collected to measure LPL activity. Subsequent to LPL displacement, hearts were used for heparin–sepharose chromatography. To evaluate the effect of Angptl-4 on LPL at the vascular lumen, hearts from control and D55 animals were perfused with or without 1 ng/mL purified Angptl-4 for 1 h in a recirculating mode. Perfusates were collected and run on a heparin–sepharose column. After Angptl-4 perfusion, the hearts were perfused with heparin to release LPL activity remaining at the vascular lumen.

Isolation of cardiac myocytes. Ventricular, calcium-tolerant myocytes were prepared by a previously described procedure (31).

Treatments. The glucosidase inhibitor castanospermine (Cs; 50 mmol/L, 2 h) was used to interrupt the association between LPL and calnexin. Colocalization of LPL and calnexin was observed using immunofluorescence. LPL activity released into the medium and remaining in the myocytes was also measured. Myocytes were also exposed to 25 mmol/L glucose (high glucose [HG]) and 1.0 mmol/L palmitic acid (PA) bound to 1% BSA (HG+PA) for 2 h. Cells were then lysed and run on a heparin–sepharose column. To evaluate the impact of HG+PA on processing of newly synthesized LPL, cells were preincubated with 50 μmol/L cyclohexamide (CHX; 1 h) to inhibit protein synthesis. Subsequently, cells were washed and treated with HG+PA for another hour, and LPL activity released into the media was determined. Calnexin and LPL colocalization was also visualized at the indicated times. To study the effect of FA on *Angptl-4* expression, isolated myocytes were treated with 1.0 mmol/L PA for 4–24 h, and Angptl-4 mRNA was determined using real-time PCR. To study the direct effect of Angptl-4 on cardiomyocytes, isolated cardiomyocytes from control animals were incubated with Angptl-4 for the indicated times, and LPL activity in the media and on the cell surface (by incubating cardiomyocytes with media containing 8 units/mL heparin for 1 min) was determined. In a separate experiment, at the end of treatment, cell lysates were loaded onto a heparin–sepharose column, and dimeric LPL was determined.

Heparin–sepharose chromatography. Heparin–sepharose chromatography was carried out as described previously to separate dimeric LPL from monomers (20,27). Heart perfusates or equal amounts (total protein) of tissue homogenates or cell lysates were loaded onto a HiTrap HP column and sequentially eluted with 0.25, 0.75, 1.0, and 1.5 mol/L NaCl at 0.2 mL/min. Fractions (1 mL each) collected were used to detect LPL activity and protein by ELISA (USCNLIFE, Wuhan, China) or Western blot after trichloroacetic acid (TCA) precipitation. To determine the total amount of monomeric or dimeric LPL, fractions from 0.75 or 1.0 mol/L NaCl were combined before TCA precipitation. To determine the processing stage of dimeric LPL, aliquots from the 1.0 mol/L NaCl fractions were subjected to endoglycosidase H (endo H) digestion. Digested products of LPL were visualized by Western blotting after TCA precipitation.

Immunofluorescence. After the indicated treatments, cells were double stained with Alexa635 and Alexa488 to colocalize LPL (red) and calnexin (green), respectively. 4,6-Diamidino-2-phenylindole (DAPI) was used to stain nuclei. Slides were visualized using a confocal microscope.

In vitro inhibitory effect of Angtpl-4 on LPL activity. LPL from vascular lumen was obtained by perfusing hearts from D55 animals with heparin. Purified human Angptl-4 was incubated with perfusates containing peak LPL activity at a final concentration of 1 ng/mL, 0.1 μg/mL, and 1 μg/mL. The reaction mix was incubated at 37°C, and at the indicated times, 100 μL reaction solution was removed for measuring LPL activity.

LPL activity. LPL catalytic activity was determined by measuring the in vitro hydrolysis of a sonicated [^{3}H]triolein substrate emulsion (15). The standard assay conditions were 0.6 mmol/L glycerol tri[9,10-^{3}H]oleate (1 mCi/mmol; 1 Ci = 37 GBq), 25 mmol/L piperazine-*N*,*N*′-bis(2-ethanesulfonic acid) (pH 7.5), 0.05% (wt/vol) albumin, 50 mmol/L $MgCl_2$, and 2% (vol/vol) heat-inactivated chicken serum as a source of apo-CII. The reaction mix was incubated at 30°C for 30 min. Reaction product, sodium [^{3}H]oleate, was extracted and determined by liquid scintillation counting. Results are expressed as nmol/h/mL (perfusate, elution fraction, or media) or nmol/h/mg protein (cell lysate).

Real-time quantitative PCR. LMF1 and Angptl-4 mRNA levels were determined using SYBR Green real-time quantitative PCR (Roche, Indianapolis, IN). Primer sequences were as follows: *LMF1* forward, 5′-TGATCCTGCAGGGCACA-3′; *LMF1* reverse, 5′-GTCCAGGCGGTAGTGGTA-3′ (32); *Angptl-4* forward, 5′- CTCTGGGATCTCCACCATTT-3′; *Angptl-4* reverse, 5′-TTGGGGATCTCCGAAGCCAT-3′ (33). All values obtained were normalized to 18S ribosomal RNA.

Serum measurements. Blood samples were collected from the tail vein before termination and serum isolated. Concentrations of nonesterified fatty acid (NEFA) and TG were determined using diagnostic kits (Wako, Osaka, Japan and Stanbio, Boerne, TX). Angptl-4 was analyzed using an ELISA kit from Raybiotech (Burlington, CA).

Reagents and antibodies. DZ, STZ, PA, Cs, and CHX were obtained from Sigma (St. Louis, MO). [^{3}H]triolein was purchased from Amersham Canada (Ontario, Canada). Purified human Angptl-4 protein (Genway Biotech, San Diego, CA) is a human recombinant and 100% homologous to the 26–229 amino acid sequence of human Angptl-4. Anti-calnexin antibody was from Stressgen (Victoria, British Columbia, Canada). Anti-LPL 5D2 antibody was a gift from J. Brunzell, University of Washington (Seattle, WA). It is a monoclonal antibody recognizing LPL from different species, but not related lipases like hepatic lipase (34). Anti-rabbit True Blot was from eBioscience (San Diego, CA). All other antibodies were obtained from Santa Cruz Biotechnology (Santa Cruz, CA).

Statistical analysis. Values are means ± SE. Wherever appropriate, one-way ANOVA followed by the Bonferroni test was used to determine differences between group mean values. The level of statistical significance was set at $P < 0.05$.

RESULTS

General characteristics of the experimental animals. Injection of DZ resulted in stable hyperglycemia within 4 h. These animals also exhibited an increase in circulating levels of NEFA. Although administration of STZ at both doses produced hyperglycemia of equal intensity as that seen with DZ, only D100 animals showed a robust elevation in circulating FA and TG levels (Table 1).

Processing of LPL into an active dimeric enzyme is increased after DZ. LPL is an enzyme present in two forms based on its affinity to a heparin–sepharose column. Monomeric LPL has low affinity to the column, is predominantly eluted in 0.4–0.75 mol/L NaCl fractions, and has no catalytic activity. Active LPL is a homodimer eluted at higher concentrations of NaCl (1.0–1.5 mol/L) (20,27). We found that the majority of LPL in the heart is monomeric (eluted at 0.75 mol/L NaCl), with only ~30% of the enzyme in the form of dimers (eluted in 1.0 mol/L NaCl fractions) accounting for all of the LPL activity (Supplementary Fig. 1). Consistent with our previous studies, total LPL protein remained unchanged after acute hyperglycemia induced by DZ (Fig. 1*A*). However, when equal amounts of homogenate protein were loaded onto a heparin–sepharose column, the 1.0 mol/L fractions from DZ hearts demonstrated higher LPL activity (Fig. 1*B*) and protein (Fig. 1*C*), suggesting the presence of more dimeric LPL in these hearts.

TABLE 1
General characteristics of experimental animals

	Blood glucose (mM)	NEFA (mM)	TG (mM)
Control	6.2 ± 0.9	0.3 ± 0.1	0.5 ± 0.1
Diazoxide	26.2 ± 2.5*	1.0 ± 0.2*	0.5 ± 0.2
D55	24.6 ± 2.0*	0.4 ± 0.1	0.5 ± 0.3
D100	28.0 ± 1.8*	1.0 ± 0.3*	2.3 ± 0.5*

Blood samples were collected from the tail vein before termination, and serum was isolated by centrifugation. Serum concentrations of NEFA and TG were determined using diagnostic kits. Results are the mean ± SE of three animals in each group. *Significantly different from control, $P < 0.01$.

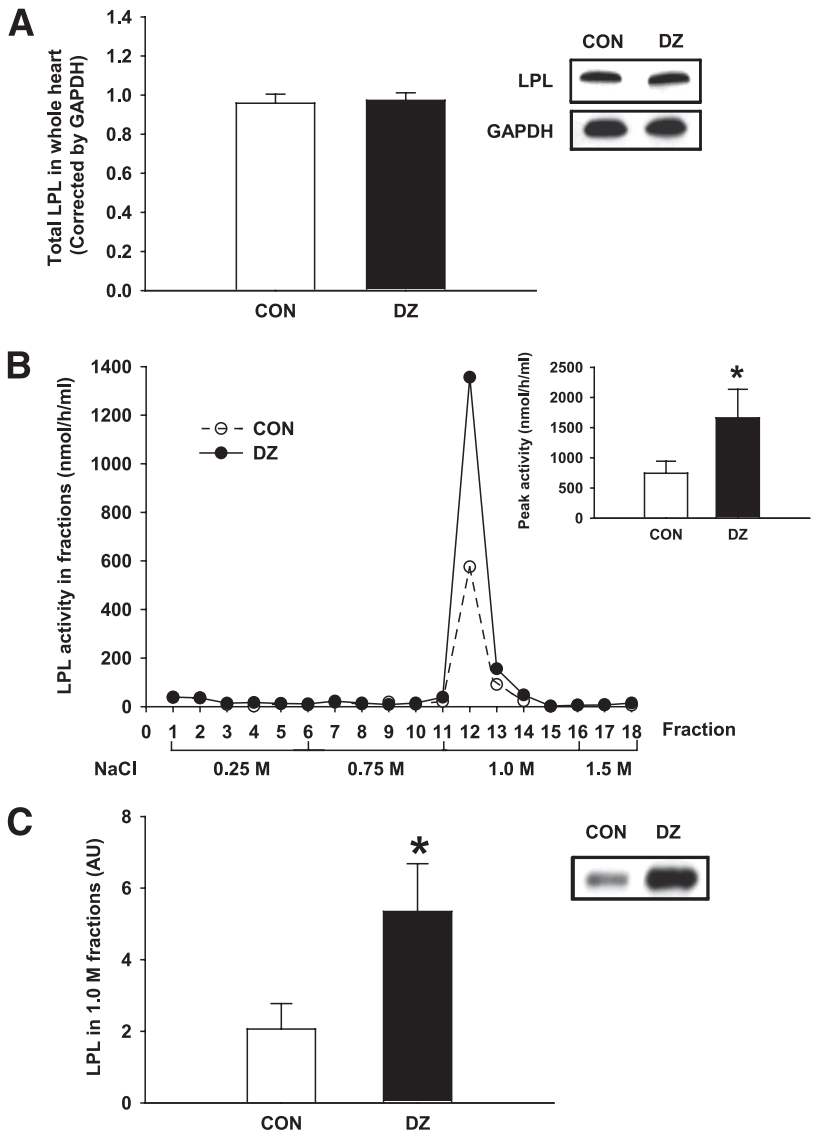

FIG. 1. Acute hyperglycemia increases cardiac LPL dimerization. Male Wistar rats were made hyperglycemic by injecting 100 mg/kg DZ i.p. Four hours after injection, animals were killed and hearts were removed. Total LPL protein expression was determined using Western blot normalized to GAPDH. Results are the mean ± SE of six animals in each group (*A*). Ventricles were lysed with 25 mmol/L ammonia buffer, pH 8.2, containing 1% Triton X-100, 0.1% SDS, 10 units/mL heparin, and protease inhibitor. Equal amounts of total protein from control (CON) and DZ heart homogenates were loaded onto a heparin–sepharose column and eluted with increasing concentrations of NaCl (0.25, 0.75, 1.0, and 1.5 mol/L). One milliliter fractions were collected and examined for LPL activity. Before the activity assay, aliquots of each fraction were diluted with equilibration buffer containing BSA to adjust NaCl concentration to 0.25 mol/L and BSA to 1 mg/mL. Elution was repeated with samples from six animals in each group, but only a representative heparin–sepharose chromatography is illustrated (*B*). Peak LPL activity is presented as mean ± SE from six animals in each group (*B*, *inset*). Fractions with LPL activity (1.0 mol/L) were combined and precipitated by TCA before Western blot for LPL was carried out (*C*). Results are the mean ± SE of six animals in each group. *Significantly different from control, $P < 0.05$. AU, arbitrary units.

Dimeric LPL could be located either at the vascular lumen or within cardiomyocytes. To determine vascular LPL, hearts were perfused with heparin, and LPL activity was measured in the perfusate. DZ hearts possessed increased LPL activity at this site (Fig. 2*A*). After stripping of the dimeric enzyme from the vascular lumen with heparin, hearts with predominantly myocyte LPL were then subjected to a heparin–sepharose column. Interestingly, in addition to the vascular lumen, DZ hearts also harbored increased dimeric LPL in cardiomyocytes (Fig. 2*B*, *lane 1* vs. *3*). Maturation of LPL including dimerization occurs within the ER of cardiomyocytes. To further localize myocyte LPL dimers, we used endo H to digest dimeric LPL. Endo H cleaves the glycan chains of LPL based on their processing stages in different cellular organelles; the 57- and 55-kDa products represent LPL that has either passed or is present within Golgi apparatus, respectively, whereas the 52-kDa band refers to LPL undergoing processing inside the ER (19,20). Interestingly, DZ hearts had a higher proportion of dimeric LPL at a post-ER processing stage (Fig. 2*B*, *lane 2* vs. *4*), implicating augmented maturation of LPL after DZ. To examine whether this is due to acute exposure to a hyperglycemic and hyperlipidemic environment seen in DZ animals, isolated cardiomyocytes were incubated with HG+PA for 2 h. Using the same conditions, we have previously found an accelerated LPL trafficking from Golgi to the myocyte surface. HG+PA also increased dimerization of LPL (Fig. 2*C*), indicating that processing of LPL could be a prerequisite for trafficking.

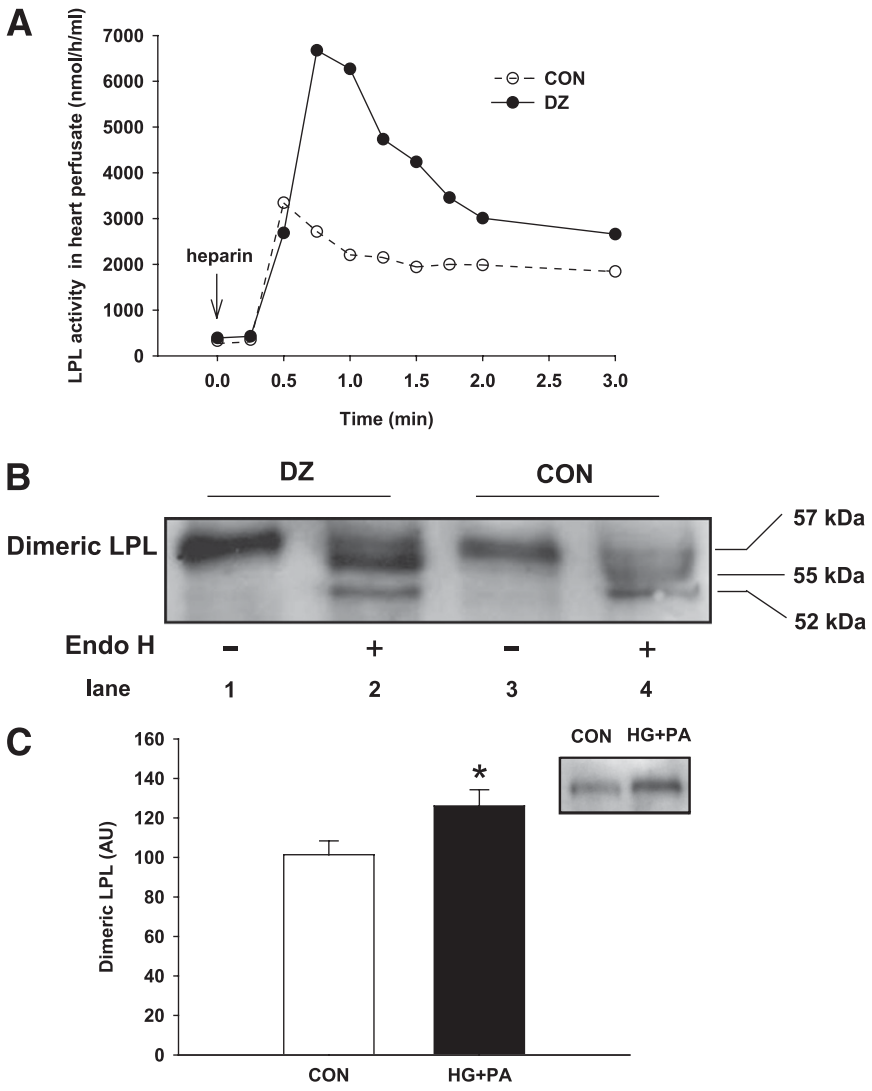

FIG. 2. Increased LPL dimers are present in cardiomyocytes from DZ animals and cells acutely exposed to HG and PA. Four hours after injection of DZ, hearts were isolated and perfused with heparin (5 units/mL), and fractions of perfusate at the indicated times were analyzed for LPL activity (*A*). Subsequent to heparin perfusion and detachment of vascular LPL, heart homogenates were subjected to heparin–sepharose elution to isolate LPL dimers (in the 1.0 mol/L NaCl elutions). These fractions were combined, digested with (+) or without (−) endo H for 20 h, and concentrated by TCA precipitation, and LPL protein was determined by Western blot (*B*). Isolated cardiac myocytes were plated on laminin-coated 60 × 15-mm tissue culture dishes and treated with PA (1 mmol/L bound to 1% BSA) and 25 mmol/L glucose (HG+PA) for 2 h. Media containing 1% BSA was used as control (CON). Cellular dimeric LPL was determined by running cell lysates onto a heparin–sepharose column, and fractions eluted at 1.0 mol/L NaCl were used to determine LPL protein by Western blot (*C*). Results are the mean ± SE of five repeated experiments using different animals. *Significantly different from control, $P < 0.05$. AU, arbitrary units.

Calnexin is required for LPL processing and is enhanced after diabetes. LPL is a glycan protein whose processing into active dimers requires its association with ER-resident chaperones like calnexin/calreticulin to allow proper folding. Using immunofluorescence, LPL and calnexin were found to be intensively colocalized at the perinuclear region (Fig. 3*A*). LPL association with this chaperone was further confirmed by immunoprecipitation (Fig. 3*A*, *inset*). Cs is a glucosidase inhibitor that blocks trimming of LPL glycan chains, such that it cannot be recognized by calnexin (22). Using Cs, we were able to inhibit the association between LPL and calnexin; a complete absence of the perinuclear colocalization of these proteins was observed (Fig. 3*B*, *inset*). This hindered LPL secretion and processing; both secreted (Fig. 3*B*) and intracellular (Fig. 3*C*) LPL activity declined in the presence of Cs, likely due to reduced LPL dimerization (Fig. 3*C*, *inset*). To determine whether HG+PA augmented LPL processing by affecting the association between calnexin and newly synthesized LPL, cardiomyocytes were pretreated with the protein synthesis inhibitor CHX. After 1 h, as a result of no newly synthesized LPL entry into the ER, CHX abolished the association between LPL and calnexin (Fig. 3*D*, *inset 2*). Upon removal of CHX and renewal of protein synthesis, association between newly synthesized LPL and calnexin was visualized in the presence or absence of HG+PA. One hour after re-entry of LPL into the ER, newly synthesized LPL was observed colocalized with calnexin at the perinuclear region (Fig. 3*D*, *inset 3*). However, in contrast to Cs, even though HG+PA attenuated this colocalization (Fig. 3*D*, *inset 4*), more LPL was observed present at the cell surface, suggesting that more enzyme had completed processing under these conditions. Increased LPL processing was also reflected by more active LPL being released into the media (Fig. 3*D*).

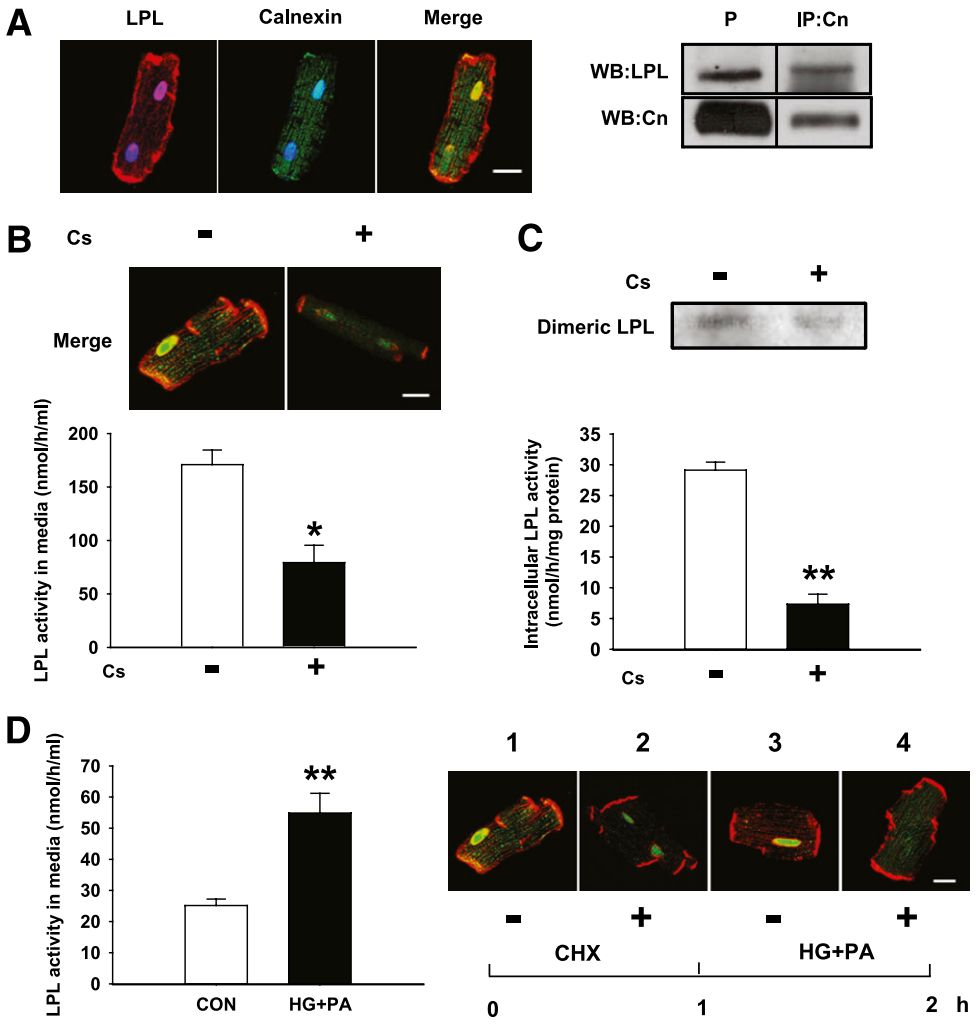

FIG. 3. LPL maturation requires calnexin and is enhanced by HG and PA. Plated myocytes from control (CON) were immunostained with LPL (red) and calnexin (green). DAPI was used to stain the nuclei (blue), and colocalization of LPL and calnexin was visualized (Merge, yellow) (*A*). Cells were lysed with CHAPS lysis buffer (50 mmol/L HEPES buffer, pH 7.5, containing 1% CHAPS, 200 mmol/L NaCl, and protease inhibitor). Cell lysate of cardiomyocytes from control animals were immunoprecipitated using anti-calnexin (IP:Cn) antibody overnight at 4°C. The immunocomplex was captured by anti-rabbit Ig IP beads and immunoblotted for LPL. Direct Western blot (WB) of cell lysate was carried out as a positive control (P) (*A*, *inset*). Dividing lines on Western blot images describe where bands from the same blot have been juxtaposed. Isolated myocytes were incubated in the presence or absence of Cs for 2 h. At the end of treatment, colocalization of LPL and calnexin was visualized (*B*, *inset*). LPL activity released into the medium (*B*) and remaining in the myocytes (*C*) was measured. Treated cardiomyocytes were also loaded onto a heparin–sepharose column to determine the amount of dimeric LPL (*C*, *inset*). Results are the mean ± SE of three repeated experiments using different animals. *Significantly different from control, $P < 0.05$. **Significantly different from control, $P < 0.01$. Isolated myocytes were preincubated with 50 μmol/L CHX for 1 h. After sufficient washing to remove CHX, cells were treated with HG+PA or BSA only (CON) for another hour. LPL activity released into the media within this hour was measured (*D*). Results are the mean ± SE of three repeated experiments using different animals. **Significantly different from control, $P < 0.05$. Cells were also fixed with 4% paraformaldehyde before (*D*, *inset 1*) or after (*inset 2*) preincubation with CHX, and also after treatment with (*inset 3*) or without (*inset 4*) HG+PA. Colocalization of LPL and calnexin (yellow) in these conditions was visualized by immunofluorescence. Scale bar, 25 μm. (A high-quality digital representation of this figure is available in the online issue.)

To examine LPL processing subsequent to chronic diabetes, 55 mg/kg of STZ was administered to generate "moderate diabetes". Similar to DZ, although chronic diabetes did not increase total LPL protein (data not shown), D55 hearts also demonstrated higher amounts of dimeric LPL (Fig. 4*A*). The importance of calnexin in LPL processing is also suggested in D55 hearts; augmented LPL dimerization in these hearts was accompanied by increased calnexin expression (Fig. 4*B*). However, we did not observe the same increase in calnexin when cardiomyocytes were acutely exposed to HG+PA (data not shown). Another crucial factor for LPL dimerization, *LMF1*, was found to be unchanged after D55 (Supplementary Fig. 2). Overall, our data suggest that after diabetes, more LPL is processed into its active dimeric form, which appears to involve the ER chaperone calnexin.

Severe diabetes reduces dimeric LPL in the heart with increased expression of Angptl-4. Increasing the dose of STZ to 100 mg/kg (D100) produced hyperglycemia similar to that observed in D55 animals. However, unlike D55, D100 animals developed severe hyperlipidemia (Table 1). Additionally, in contrast to D55, D100 animals showed a decline in dimeric LPL, both in the whole heart (Fig. 5*A*) and at the vascular lumen (Fig. 5*B*). This effect on LPL was not a result of decreased calnexin expression in D100 (Fig. 5*C*) but was accompanied by a robust increase in Angptl-4 serum concentrations (Fig. 5*D*). Furthermore, cardiac expression of Angptl-4 protein (Fig. 5*E*) and mRNA (Fig. 5*E*, *inset*) was also found to be higher in D100 animals.

Angptl-4 is capable of inhibiting LPL activity and its expression is stimulated by FA. To test the direct inhibitory effect of Angptl-4 on LPL, dimeric LPL collected

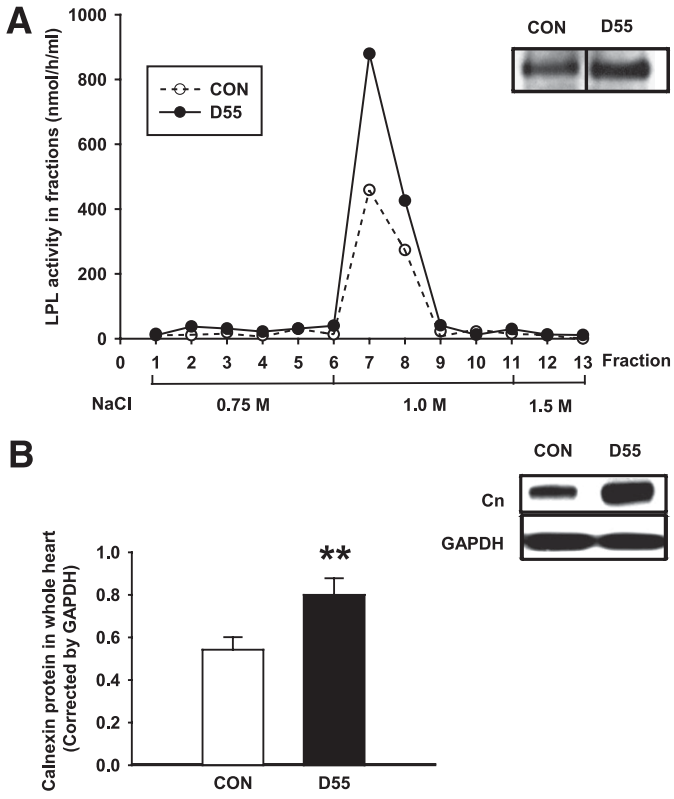

FIG. 4. Chronic diabetes also augments LPL processing with increased expression of calnexin. For chronic diabetes, animals were injected with 55 mg/kg STZ (D55) and after 4 days, hearts were removed. Equal amounts of total protein from control (CON) and D55 heart homogenates were loaded onto a heparin–sepharose column, prewashed with 0.25 mol/L NaCl, and eluted with 0.75, 1.0, and 1.5 mol/L NaCl. LPL activity in each fraction was analyzed (*A*), and fractions from 1.0 mol/L NaCl (containing LPL dimers) were combined to determine LPL amount by Western blot after TCA precipitation. Only a representative chromatography (*A*) and blot of LPL (*A*, *inset*) are shown from five repeated experiments. Dividing lines on Western blot images describe where bands from the same blot have been juxtaposed. Calnexin protein expression (Cn) in CON and D55 hearts was determined by Western blot and normalized to GAPDH (*B*). Results are the mean ± SE of five animals in each group. **Significantly different from control, $P < 0.01$.

from the vascular lumen of D55 animals was incubated with purified Angptl-4 in vitro. The inhibition of LPL activity by Angptl-4 was fast (within 15 min) and dose dependent, with 1 μg/mL Angptl-4 inhibiting ~85% of the enzyme activity at 2 h (Fig. 6*A*). It should be noted that the serum concentration of Angptl-4 in D100 animals (1 ng/mL) was effective in inhibiting ~20% of LPL activity in vitro (Fig. 6*A*). When this concentration of Angptl-4 was perfused through D55 hearts for 1 h, LPL activity remaining at the vascular lumen was reduced (Fig. 6*C*). Interestingly, this reduction in LPL activity correlated with an increased appearance of monomeric LPL in the perfusion buffer (Fig. 6*B*) and a decline in dimeric LPL remaining at the coronary lumen (Fig. 6*C*, *inset*), suggesting that the inhibitory action of Angptl-4 on LPL is through the conversion of dimeric LPL into monomers, which in turn reduces its affinity to the binding sites at the vascular lumen. This inhibitory effect of Angptl-4 was also observed in isolated hearts (Supplementary Fig. 3*A*) and cardiomyocytes (Supplementary Fig. 3*B* and *C*) from control animals. To duplicate the elevated serum NEFA level seen in D100 animals, isolated cardiomyocytes were treated with 1.0 mmol/L PA for 4–24 h. Within 4 h of exposure to PA, Angptl-4 mRNA did not change significantly. However, at 12 h, increase in Angptl-4 mRNA was observed, an effect that was even more dramatic after a 24-h exposure to PA (Fig. 6*D*).

DISCUSSION

The majority of FA provided to the heart comes from breakdown of circulating TG, a process catalyzed by LPL located at the vascular lumen (35). In mice with cardiac overexpression of LPL, excess lipid uptake is evident, with development of dilated cardiomyopathy (36). Paradoxically, chronic cardiac depletion of LPL is also associated with a decrease in cardiac ejection fraction (37). Thus, cardiac LPL is of crucial importance for regulating lipid metabolism in hearts, and disturbing its innate function is sufficient to cause cardiomyopathy. Diabetes is a unique metabolic disorder during which either an increase (moderate type 1 diabetes) or decrease (severe type 1 diabetes) in vascular LPL activity is observed. Data from this study suggest that after acute hyperglycemia and moderate diabetes, more LPL is processed into an active dimeric form, whereas severe diabetes is associated with increased conversion of LPL into inactive monomers (Fig. 7).

In type 1 diabetic patients, insulin supplementation can never mimic the exquisite control of glucose by pancreatic insulin seen in normal individuals. Multiple finger pricks and insulin injections (three to four per day) mean poor patient compliance, repeated exposure to bouts of inadequate glucose control (and a shift in cardiac metabolism), and cardiovascular disease in the long term. To imitate this poorly controlled type 1 diabetic patient exposed to acute hyperglycemia, we used DZ. Measurement of LPL protein expression in the heart revealed no change after acute hyperglycemia. However, the drawback with this measurement is that it does not distinguish active LPL from its inactive monomeric form. Using the heparin–sepharose column, our data for the first time show that acute hyperglycemia can indeed increase the amount of dimeric LPL in the heart. We are unaware of a similar increase in dimeric LPL in other physiology or pathology. In fact, the reverse is often seen with lipid metabolism disorders. In one case of human familial LPL deficiency, the Tyr262→His mutation of the *LPL* gene results in shifting of dimeric LPL to monomers (38). In addition, in cell lines derived from animals with a mutation (*cld*) that impairs posttranslational processing of LPL, a significant amount of inactive LPL is produced as aggregated monomers (21). The increased dimeric LPL in the whole heart after acute hyperglycemia correlated well with the elevated LPL activity at the vascular lumen. Our data suggest that after a rapid rise in circulating glucose, a unique augmentation in LPL dimerization contributes toward increased coronary enzyme, delivering more FA to the heart.

After stripping of dimeric LPL from the vascular lumen, more LPL dimers were still evident in the myocytes from acute diabetic animals. These dimeric LPL could be located inside the ER, Golgi, or secretion vesicles or at the myocyte surface. Interestingly, the majority of dimeric LPL displayed resistance to endo H digestion (20). This suggested that after DZ, LPL processing is very efficient, with more LPL completing its maturation in the ER before moving to the Golgi. Early processing of LPL into a conformation competent for dimerization is suggested to involve chaperones like calreticulin/calnexin. For example, in a transfected sf21 cell line, folding/dimerization of human LPL is only promoted when calreticulin is coexpressed (39). In addition, the impaired LPL processing

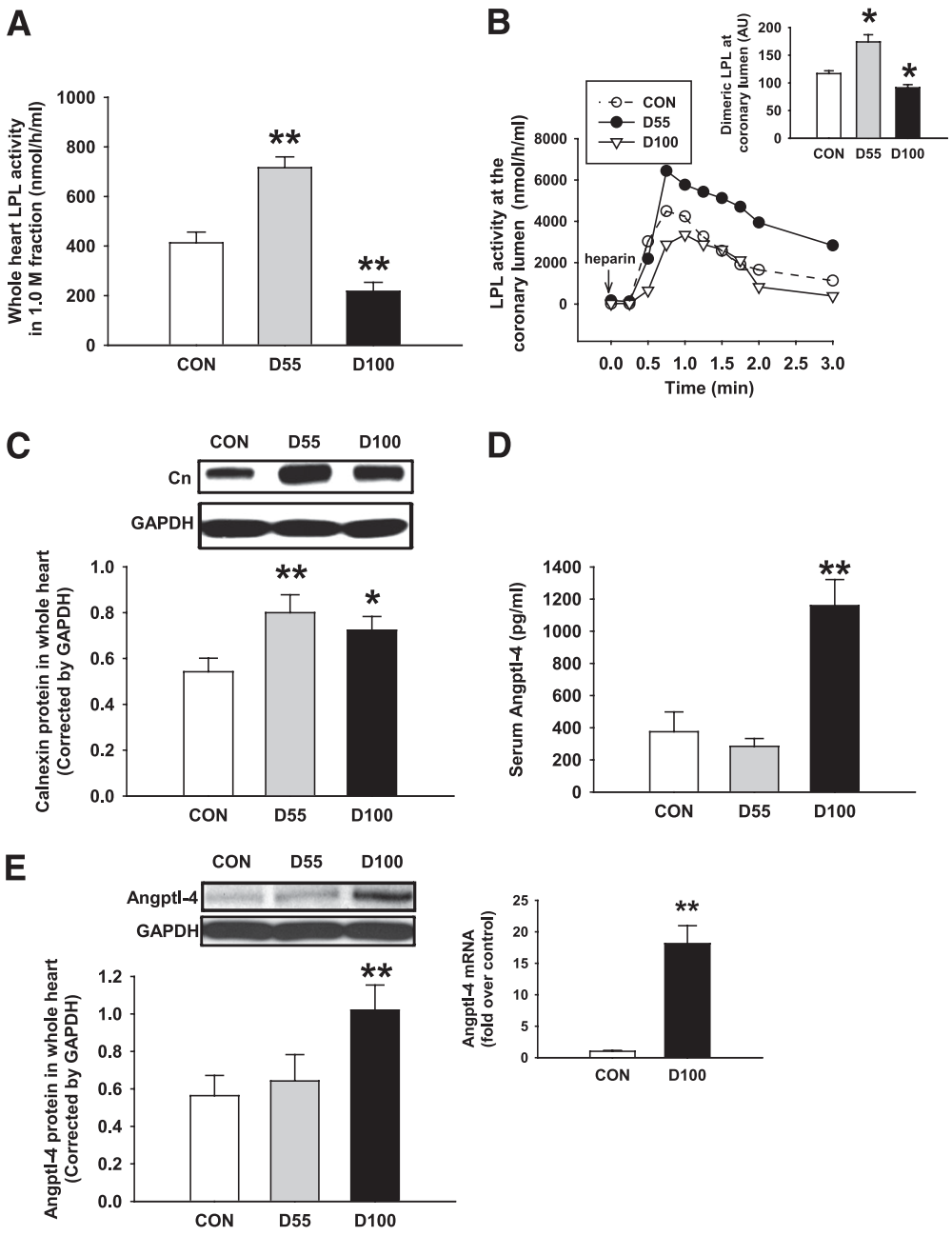

FIG. 5. Severe diabetes reduces LPL dimers with an increase in Angptl-4. Animals were made moderately or severely diabetic by injecting STZ at a dose of 55 (D55) or 100 mg/kg (D100), respectively, and kept for 4 days. Hearts were isolated and equal amounts of homogenate protein from control (CON), D55, and D100 were loaded onto a heparin–sepharose column and eluted with increasing concentrations of NaCl. LPL activity in the 1.0 mol/L fractions was measured, and peak activity presented as mean ± SE of five animals in each group (*A*). In a separate experiment, hearts from CON, D55, and D100 were perfused with heparin (5 units/mL), perfusates were collected at the indicated times, and LPL activity was determined (*B*, representative graph). These perfusates at the indicated times were pooled and loaded onto a heparin–sepharose column. Dimeric LPL in the 1.0 mol/L fractions was determined using TCA precipitation followed by Western blot (*B*, *inset*). Results are the mean ± SE of three animals in each group. *Significantly different from control, $P < 0.05$. Heart homogenates from CON, D55, and D100 were also used for Western blot to detect calnexin (Cn) (*C*) or Angptl-4 (*E*) protein expressions normalized by GAPDH. Serum samples were collected from the different groups to detect Angptl-4 using an ELISA assay (*D*). Angptl-4 mRNA expression from CON and D100 hearts was analyzed by real-time quantitative PCR. Gene expression was evaluated by normalizing to 18S-ribosomal RNA and plotted as fold over control (*E*, *inset*). Results are the mean ± SE of five animals in each group. *Significantly different from control, $P < 0.05$. **Significantly different from control, $P < 0.01$.

seen in *cld/cld* mice is related to a decreased expression of calnexin (40). In our study, LPL in control cardiomyocytes was found associated with calnexin. As interruption of this association by Cs hindered LPL dimerization and secretion, our data imply that calnexin is important for LPL processing in the heart.

We have previously found that HG+PA increased LPL trafficking from the Golgi to myocyte surface (12,15). The current data suggest that HG and PA are also responsible for enhanced LPL dimerization. To test whether the effect of an acute diabetic environment on LPL processing is not a transient response, we turned to a more chronic diabetes model using D55 animals. A significant increase in the amount of LPL dimers correlated with an increased expression of calnexin in D55 hearts. As no change in *LMF1* gene expression was observed, our data suggest that

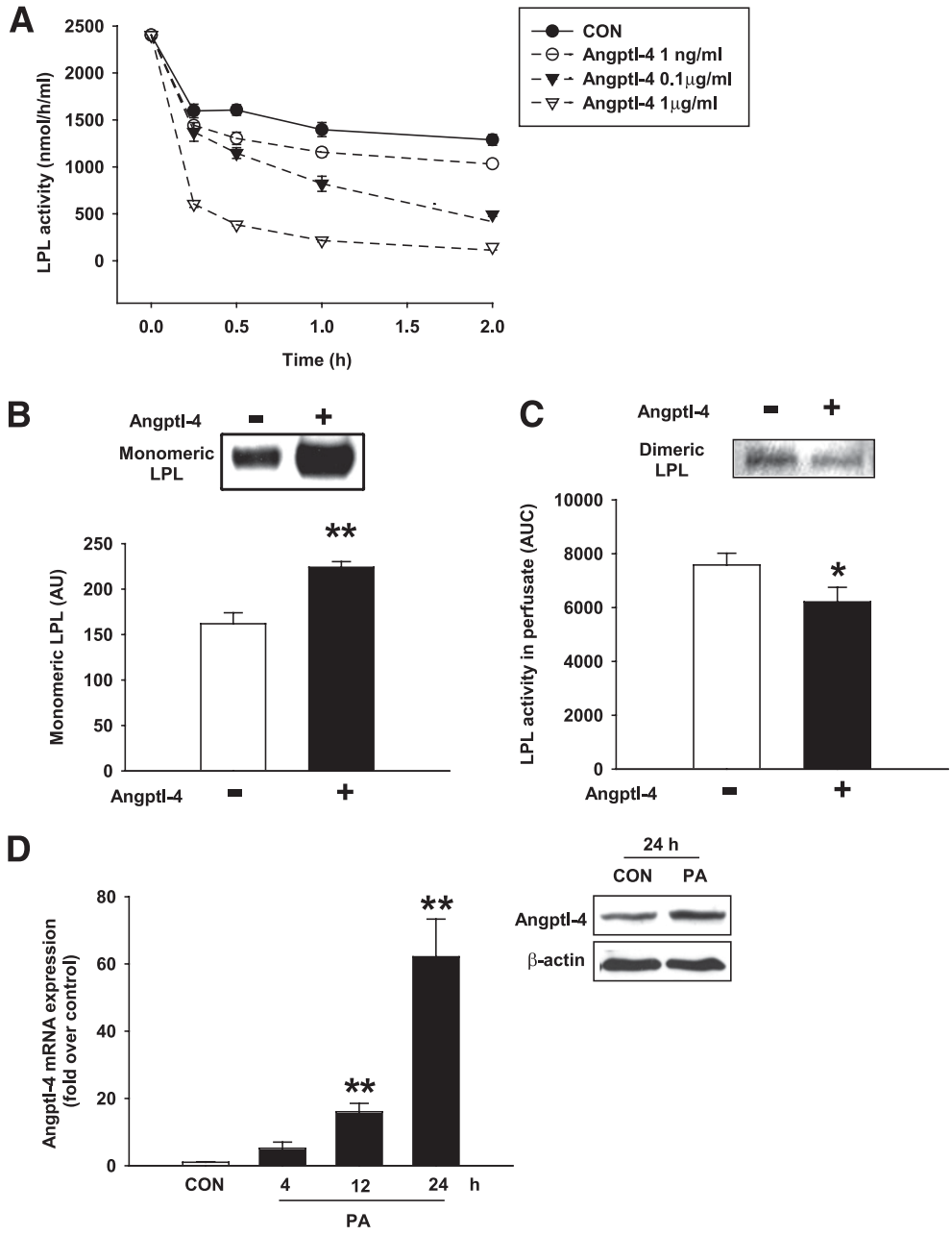

FIG. 6. Angptl-4, which reduces LPL activity, is upregulated by FA. Hearts from D55 animals were perfused with heparin to release LPL at the vascular lumen. Fractions with peak LPL activity were then incubated with purified human Angptl-4 at a final concentration of 1 ng/mL, 0.1 μg/mL, and 1 μg/mL. Reaction mix was incubated at 37°C and LPL activity at the indicated times was determined (*A*). Results are the mean ± SE from three repeated experiments. Hearts from D55 animals were also directly perfused with or without 1 ng/mL purified Angptl-4 for 1 h. Perfusion buffer was collected at the end of this period. Monomeric LPL released into the perfusates was isolated by collecting the 0.75 mol/L fractions from the heparin–sepharose column and quantified by Western blot (*B*). After Angptl-4 perfusion, hearts were subsequently perfused with 5 units/mL heparin to release LPL activity remaining at the vascular lumen. LPL activity in the perfusate is expressed as area under curve over the 3-min perfusion (*C*). These perfusates over 3 min were pooled and loaded onto a heparin–sepharose column to visualize dimeric LPL in the 1.0 mol/L fractions (*C*, *inset*). Results are the mean ± SE of three animals in each group. Isolated cardiomyocytes were incubated with 1.0 mmol/L PA for 4, 12, or 24 h. mRNA expression of Angptl-4 was quantified by real-time PCR and compared with control (CON) treated with 1% BSA (*D*). Protein expression of Angptl-4 after 24-h incubation with PA is illustrated in the *inset*. Results are the mean ± SE of five repeated experiments using different animals. *Significantly different from control, $P < 0.05$. **Significantly different from control, $P < 0.01$. AU, arbitrary units; AUC, area under curve.

chronic diabetes may have a profound impact on the early processing events of LPL dimerization. It is possible that the increased calnexin expression after chronic diabetes is related to the unfolded protein response (UPR), an adaptive mechanism that augments protein processing efficiency after ER stress (41). One of the three well-defined arms of UPR includes up-regulation of ER chaperone expression through activation of inositol-requiring kinase 1 (IRE-1) on the ER membrane (42,43). It should be noted that acute exposure to HG+PA had no effect on calnexin expression. Nevertheless, this environment could still alter the processing efficiency of LPL by affecting chaperone activity and accessibility in the ER through calcium and extracellular signal–regulated kinase (ERK-1). Calcium is an important

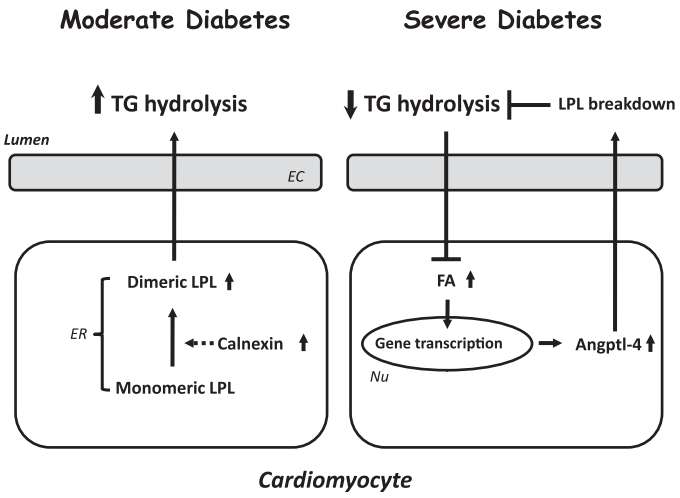

FIG. 7. Moderate and severe diabetes have a differential impact on LPL at the coronary lumen. In moderate diabetes, more monomeric LPL is processed into dimeric, catalytically active enzyme with the help of the ER chaperone calnexin. This increases LPL at the vascular lumen, breaking down more circulating TG to deliver increased FA to the heart when glucose utilization is compromised. In severe diabetes, when FA are excessive, an FA-induced expression of Angptl-4 leads to conversion of LPL to inactive monomers at the coronary lumen to impede TG hydrolysis. EC, endothelial cells; Nu, nucleus.

cofactor for protein folding in the ER, facilitating LPL dimerization, and can also impact the structural stability and substrate recognition of calnexin (44,45). ERK-1, activated in an IRE-dependent manner, can directly phosphorylate calnexin at Ser563, resulting in its recruitment to ribosomes, potentially rendering it more accessible to newly synthesized proteins (46,47). The role of calcium and ERK-1 on LPL maturation, and how diabetes could potentially alter LPL processing through these pathways, requires investigation.

In contrast to D55, D100 animals have a more profound loss of pancreatic β-cells and reduction in circulating insulin. Under these conditions, excessive lipolysis and hepatic lipoprotein secretion increases serum FA and TG, respectively. Thus, these doses of STZ represent a continuum of poor glycemic control, from moderate (D55) to severe (D100). To avoid lipid overload, LPL activity at the coronary lumen decreased in D100 hearts, and this could be due to enzyme inactivation by conversion from a dimeric to monomeric conformation (26). Angptl-4, identified to bring about this conversion, is expressed in various tissues, including white adipose tissue, liver, heart, and skeletal muscle (48). This secreted protein can function in circulation, breaking down vascular LPL (49). Our data, for the first time, report a robust increase of Angptl-4 protein, both in the serum and heart tissue from D100 animals, an effect that was not seen in D55. Given that the serum concentration of Angptl-4 in D100 was capable of inhibiting the activity of vascular LPL released from D55 hearts in vitro, we assumed that introduction of Angptl-4 to D55 hearts would give these hearts a D100 phenotype. Indeed, a drop of LPL activity was observed at the vascular lumen in D55 hearts perfused with Angptl-4, an effect that correlated well with the inhibitory efficiency in vitro. The reduction of coronary LPL activity could be due to the increased conversion of dimeric LPL into monomers, with subsequent detachment from the vascular binding sites. This effect of Angptl-4 was also evident in control hearts. Long chain FA, through activation of proliferator-activated receptor δ, has been reported to increase the transcription of *Angptl-4* in skeletal muscle cells (50). In our study, as *Angptl-4* expression in cardiomyocytes was also upregulated after exposure to PA (more than 4 h), the decrease of LPL in D100 could be through an FA–Angptl-4 pathway. As this effect was absent in DZ that had short term hyperlipidemia (less than 4 h), our data suggest that "turning off" LPL requires prolonged exposure to FA. Whether the increased expression of Angptl-4 seen in D100 hearts could contribute toward inhibition of LPL at the coronary lumen is currently unknown. Nevertheless, purified Angptl-4 was capable of directly inhibiting LPL in or on cardiomyocytes. In addition, in mice overexpressing Angptl-4 specifically in the heart, a reduced cardiac LPL activity was found without affecting this enzyme in other LPL-expressing tissues, implying a tight link between tissue-specific Angptl-4 and local or proximal vascular LPL activity (48).

In summary, after diabetes, recruitment of LPL to the vascular lumen could represent an immediate compensatory response to guarantee FA supply. In moderate type 1 diabetes, an exaggerated LPL processing to dimeric, catalytically active enzyme increases vascular LPL, delivering more FA to the heart when glucose utilization is compromised. In severe diabetes, FA-induced expression of Angptl-4 leads to conversion of LPL to inactive monomers at the coronary lumen to impede TG hydrolysis and FA supply. We suggest that both compensatory processes that alter the innate function of LPL at the vascular lumen during diabetes could be the forerunner for cardiomyopathy seen with this disease.

Limitations. When examining LPL in humans, heparin has been used to displace LPL, and either a decrease or no change in its activity has been reported in type 1 diabetic patients. As this approach releases LPL from other tissues, including skeletal muscle and adipose tissue, it is incapable of establishing cardiac LPL content. However, even if heart homogenates from patients with diabetes were used, it would still be inappropriate, as it would reflect total cardiac LPL and not the functional pool of enzyme at the coronary lumen. The animal models used in this study may not perfectly mimic the clinical condition. Nevertheless, they allowed us to distinguish functional LPL from total enzyme, and uncovered how inadequate glycemic control could lead to cardiovascular disease through manipulation of LPL-governed lipid metabolism.

ACKNOWLEDGMENTS

This study was supported by an operating grant from the Canadian Diabetes Association. P.P., F.W., and M.S.K. are the recipients of Doctoral Student Research Awards from the Canadian Diabetes Association.

No potential conflicts of interest relevant to this article were reported.

Y.W. conceived the idea, generated most data, and wrote the manuscript. P.P., F.W., M.S.K., and A.A. helped with obtaining some data. B.R. helped with writing the manuscript.

REFERENCES

1. Akasha AA, Sotiriadou I, Doss MX, et al. Entrapment of embryonic stem cells-derived cardiomyocytes in macroporous biodegradable microspheres: preparation and characterization. Cell Physiol Biochem 2008;22:665–672
2. An D, Rodrigues B. Role of changes in cardiac metabolism in development of diabetic cardiomyopathy. Am J Physiol Heart Circ Physiol 2006;291:H1489–H1506

3. Lopaschuk GD, Ussher JR, Folmes CD, Jaswal JS, Stanley WC. Myocardial fatty acid metabolism in health and disease. Physiol Rev 2010;90:207–258
4. Rodrigues B, Cam MC, McNeill JH. Myocardial substrate metabolism: implications for diabetic cardiomyopathy. J Mol Cell Cardiol 1995;27:169–179
5. Atkinson LL, Fischer MA, Lopaschuk GD. Leptin activates cardiac fatty acid oxidation independent of changes in the AMP-activated protein kinase-acetyl-CoA carboxylase-malonyl-CoA axis. J Biol Chem 2002;277:29424–29430
6. Saddik M, Lopaschuk GD. Triacylglycerol turnover in isolated working hearts of acutely diabetic rats. Can J Physiol Pharmacol 1994;72:1110–1119
7. Tannock LR, Chait A. Lipoprotein-matrix interactions in macrovascular disease in diabetes. Front Biosci 2004;9:1728–1742
8. Blanchette-Mackie EJ, Masuno H, Dwyer NK, Olivecrona T, Scow RO. Lipoprotein lipase in myocytes and capillary endothelium of heart: immunocytochemical study. Am J Physiol 1989;256:E818–E828
9. Camps L, Reina M, Llobera M, Vilaró S, Olivecrona T. Lipoprotein lipase: cellular origin and functional distribution. Am J Physiol 1990;258:C673–C681
10. Eckel RH. Lipoprotein lipase. A multifunctional enzyme relevant to common metabolic diseases. N Engl J Med 1989;320:1060–1068
11. Enerbäck S, Gimble JM. Lipoprotein lipase gene expression: physiological regulators at the transcriptional and post-transcriptional level. Biochim Biophys Acta 1993;1169:107–125
12. Kim MS, Wang F, Puthanveetil P, et al. Protein kinase D is a key regulator of cardiomyocyte lipoprotein lipase secretion after diabetes. Circ Res 2008;103:252–260
13. Kim MS, Wang F, Puthanveetil P, et al. Cleavage of protein kinase D after acute hypoinsulinemia prevents excessive lipoprotein lipase-mediated cardiac triglyceride accumulation. Diabetes 2009;58:2464–2475
14. Sambandam N, Abrahani MA, St Pierre E, Al-Atar O, Cam MC, Rodrigues B. Localization of lipoprotein lipase in the diabetic heart: regulation by acute changes in insulin. Arterioscler Thromb Vasc Biol 1999;19:1526–1534
15. Kim MS, Kewalramani G, Puthanveetil P, et al. Acute diabetes moderates trafficking of cardiac lipoprotein lipase through p38 mitogen-activated protein kinase-dependent actin cytoskeleton organization. Diabetes 2008;57:64–76
16. Garfinkel AS, Kempner ES, Ben-Zeev O, Nikazy J, James SJ, Schotz MC. Lipoprotein lipase: size of the functional unit determined by radiation inactivation. J Lipid Res 1983;24:775–780
17. Peterson J, Fujimoto WY, Brunzell JD. Human lipoprotein lipase: relationship of activity, heparin affinity, and conformation as studied with monoclonal antibodies. J Lipid Res 1992;33:1165–1170
18. Wong H, Yang D, Hill JS, Davis RC, Nikazy J, Schotz MC. A molecular biology-based approach to resolve the subunit orientation of lipoprotein lipase. Proc Natl Acad Sci USA 1997;94:5594–5598
19. Ben-Zeev O, Doolittle MH, Davis RC, Elovson J, Schotz MC. Maturation of lipoprotein lipase. Expression of full catalytic activity requires glucose trimming but not translocation to the cis-Golgi compartment. J Biol Chem 1992;267:6219–6227
20. Ben-Zeev O, Mao HZ, Doolittle MH. Maturation of lipoprotein lipase in the endoplasmic reticulum. Concurrent formation of functional dimers and inactive aggregates. J Biol Chem 2002;277:10727–10738
21. Briquet-Laugier V, Ben-Zeev O, White A, Doolittle MH. cld and lec23 are disparate mutations that affect maturation of lipoprotein lipase in the endoplasmic reticulum. J Lipid Res 1999;40:2044–2058
22. Carroll R, Ben-Zeev O, Doolittle MH, Severson DL. Activation of lipoprotein lipase in cardiac myocytes by glycosylation requires trimming of glucose residues in the endoplasmic reticulum. Biochem J 1992;285:693–696
23. Péterfy M, Ben-Zeev O, Mao HZ, et al. Mutations in LMF1 cause combined lipase deficiency and severe hypertriglyceridemia. Nat Genet 2007;39:1483–1487
24. Peterson J, Bihain BE, Bengtsson-Olivecrona G, Deckelbaum RJ, Carpentier YA, Olivecrona T. Fatty acid control of lipoprotein lipase: a link between energy metabolism and lipid transport. Proc Natl Acad Sci USA 1990;87:909–913
25. Bengtsson G, Olivecrona T. Lipoprotein lipase. Mechanism of product inhibition. Eur J Biochem 1980;106:557–562
26. Sukonina V, Lookene A, Olivecrona T, Olivecrona G. Angiopoietin-like protein 4 converts lipoprotein lipase to inactive monomers and modulates lipase activity in adipose tissue. Proc Natl Acad Sci USA 2006;103:17450–17455
27. Yau MH, Wang Y, Lam KS, Zhang J, Wu D, Xu A. A highly conserved motif within the NH2-terminal coiled-coil domain of angiopoietin-like protein 4 confers its inhibitory effects on lipoprotein lipase by disrupting the enzyme dimerization. J Biol Chem 2009;284:11942–11952
28. Pulinilkunnil T, Qi D, Ghosh S, et al. Circulating triglyceride lipolysis facilitates lipoprotein lipase translocation from cardiomyocyte to myocardial endothelial lining. Cardiovasc Res 2003;59:788–797
29. Foy JM, Furman BL. Effect of single dose administration of diuretics on the blood sugar of alloxan-diabetic mice or mice made hyperglycaemic by the acute administration of diazoxide. Br J Pharmacol 1973;47:124–132
30. Pratz J, Mondot S, Montier F, Cavero I. Effects of the K+ channel activators, RP 52891, cromakalim and diazoxide, on the plasma insulin level, plasma renin activity and blood pressure in rats. J Pharmacol Exp Ther 1991;258:216–222
31. Rodrigues B, Spooner M, Severson DL. Free fatty acids do not release lipoprotein lipase from isolated cardiac myocytes or perfused hearts. Am J Physiol 1992;262:E216–E223
32. Forcheron F, Basset A, Del Carmine P, Beylot M. Lipase maturation factor 1: its expression in Zucker diabetic rats, and effects of metformin and fenofibrate. Diabetes Metab 2009;35:452–457
33. Josephs T, Waugh H, Kokay I, Grattan D, Thompson M. Fasting-induced adipose factor identified as a key adipokine that is up-regulated in white adipose tissue during pregnancy and lactation in the rat. J Endocrinol 2007;194:305–312
34. Chang SF, Reich B, Brunzell JD, Will H. Detailed characterization of the binding site of the lipoprotein lipase-specific monoclonal antibody 5D2. J Lipid Res 1998;39:2350–2359
35. Voshol PJ, Rensen PC, van Dijk KW, Romijn JA, Havekes LM. Effect of plasma triglyceride metabolism on lipid storage in adipose tissue: studies using genetically engineered mouse models. Biochim Biophys Acta 2009;1791:479–485
36. Noh HL, Yamashita H, Goldberg IJ. Cardiac metabolism and mechanics are altered by genetic loss of lipoprotein triglyceride lipolysis. Cardiovasc Drugs Ther 2006;20:441–444
37. Noh HL, Okajima K, Molkentin JD, Homma S, Goldberg IJ. Acute lipoprotein lipase deletion in adult mice leads to dyslipidemia and cardiac dysfunction. Am J Physiol Endocrinol Metab 2006;291:E755–E760
38. Rouis M, Lohse P, Dugi KA, et al. Homozygosity for two point mutations in the lipoprotein lipase (LPL) gene in a patient with familial LPL deficiency: LPL(Asp9→Asn, Tyr262→His). J Lipid Res 1996;37:651–661
39. Zhang L, Wu G, Tate CG, Lookene A, Olivecrona G. Calreticulin promotes folding/dimerization of human lipoprotein lipase expressed in insect cells (sf21). J Biol Chem 2003;278:29344–29351
40. Scow RO, Schultz CJ, Park JW, Blanchette-Mackie EJ. Combined lipase deficiency (cld/cld) in mice affects differently post-translational processing of lipoprotein lipase, hepatic lipase and pancreatic lipase. Chem Phys Lipids 1998;93:149–155
41. Kennedy J, Katsuta H, Jung MH, et al. Protective unfolded protein response in human pancreatic beta cells transplanted into mice. PLoS ONE 2010;5:e11211
42. Eizirik DL, Cardozo AK, Cnop M. The role for endoplasmic reticulum stress in diabetes mellitus. Endocr Rev 2008;29:42–61
43. Ma Y, Hendershot LM. ER chaperone functions during normal and stress conditions. J Chem Neuroanat 2004;28:51–65
44. Zhang L, Lookene A, Wu G, Olivecrona G. Calcium triggers folding of lipoprotein lipase into active dimers. J Biol Chem 2005;280:42580–42591
45. Thammavongsa V, Mancino L, Raghavan M. Polypeptide substrate recognition by calnexin requires specific conformations of the calnexin protein. J Biol Chem 2005;280:33497–33505
46. Nguyên DT, Kebache S, Fazel A, et al. Nck-dependent activation of extracellular signal-regulated kinase-1 and regulation of cell survival during endoplasmic reticulum stress. Mol Biol Cell 2004;15:4248–4260
47. Chevet E, Wong HN, Gerber D, et al. Phosphorylation by CK2 and MAPK enhances calnexin association with ribosomes. EMBO J 1999;18:3655–3666
48. Yu X, Burgess SC, Ge H, et al. Inhibition of cardiac lipoprotein utilization by transgenic overexpression of Angptl4 in the heart. Proc Natl Acad Sci USA 2005;102:1767–1772
49. Ge H, Yang G, Huang L, Motola DL, Pourbahrami T, Li C. Oligomerization and regulated proteolytic processing of angiopoietin-like protein 4. J Biol Chem 2004;279:2038–2045
50. Staiger H, Haas C, Machann J, et al. Muscle-derived angiopoietin-like protein 4 is induced by fatty acids via peroxisome proliferator-activated receptor (PPAR)-delta and is of metabolic relevance in humans. Diabetes 2009;58:579–589